A MECHANISM FOR THE FORMATION AND EVOLUTION OF THARSIS AS A CONSEQUENCE OF MANTLE OVERTURN: LARGE SCALE LATERAL HETEROGENEITY IN A STABLY STRATIFIED MANTLE.

E.M. Parmentier, S.E. Zaranek, and L.T. Elkins-Tanton, Brown University, Department of Geological Sciences, Providence RI 02192 (EM_Parmentier@brown.edu).

Introduction: The Tharsis volcanic center developed very early in the recorded geologic history of Mars [1] and has remained active through most of the planet's evolution. The elevation of this global scale swell is due primarily to thickened crust [2,3]. We present a model in which Tharsis originates from the melting of a large scale mantle heterogeneity resulting from mantle overturn following fractional magma ocean solidification. This explains the early development of Tharsis and the long-lived volcanism that has occurred in this region without requiring a heat flux from the core. In this model, the strong stable stratification following overturn prevents thermal convection.

A frequently cited origin for Tharsis is decompression melting in a thermal plume originating by cooling of the core [cf. 4]. Tharsis is the only volcanic feature of comparable scale on Mars. The existence of only a single thermal plume in a planet the size of Mars may be a consequence of a solid state phase transition near the core-mantle boundary [5]. An internally generated magnetic field was present only during the very early evolution of Mars, so that if a plume exists, it must not have cooled the core sufficiently to sustain a magnetic field throughout most of the planet's evolution. A recent alternative proposal is that Tharsis originated as a large impact which determined the location of subsequent mantle upwelling and melting [6]. However, no indication of upwelling and melting beneath other large impact structures can be seen.

Magma ocean solidification and overturn: Fractional solidification of a magma ocean in which the solidus is steeper than an adiabat leads to a liquid or partly solid region overlying fully solid silicate mantle. The thickness of fully solid region increases as the magma ocean cools. We assume 1) chemical equilibrium in an adiabatic liquid or partly solid region, 2) equilibrium between each new increment of solid and remaining liquid, and 3) that the fully solid mantle retains temperature and composition along solidus. This leads to compositionally stratified mantle [7]. At pressures exceeding 14 GPa, both majorite and γ-olivine are denser than coexisting liquid. However, at lower pressures (albeit > 7.5 GPa) garnet is denser but both olivine and pyroxene are less dense than liquid. During magma ocean solidification, olivine and pyroxenes should remain suspended while garnet should segregate. The resulting mantle structure, shown in Figure 1, is gravitationally unstable due to both the garnet layer and the upward Fe-enrichment. Overturn to a stable structure with density increasing monotonically with depth, as shown, will occur on a time scale, which depending on thermally-activated creep rate, may be as short as a few Myr. For a non-monotonic pre-overturn density distribution, materials of the same density but different composition end up over the same range of depth in the upper mantle as shown in Figure 1 (right).

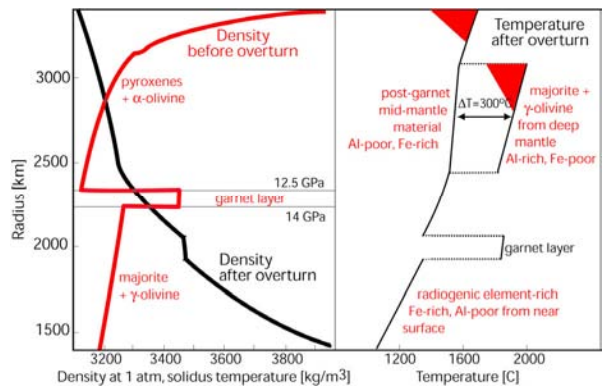

Figure 1: Density stratification (left) before and after overturn of fractionally solidified magma ocean. Temperature distribution (right) after overturn. Red shows regions of decompression melting.

During overturn mantle at its solidus temperature decompresses as it rises to shallower depth. The resulting adiabatic decompression melting provides a mechanism for generating an early crust. As shown in Figure 1, decompression melting of mantle with two different source compositions may occur. Crustal materials of these different compositions may explain the crustal dichotomy present on Mars. Overturn also brings cold mantle to the core-mantle boundary, and the conductive heating of this mantle may explain the presence of an early but brief internally generated magnetic field [8].

Overturn of a nonmontonic density distribution like that shown in Figure 1 by buoyant viscous flow creates large scale lateral heterogeneity in the overturned mantle[9] where mantle material of similar density but different composition is distributed laterally at a given depth as reflected by the form and scale flow associated with overturn. Figure 2 shows a spherical axially symmetric model of the overturn of a viscous fluid with pressure and temperature-dependent creep viscosity. In this example initial depth of material serves as a proxy for its composition; a shallower

initial depth corresponds to mantle more depleted in Al and enriched in Fe and incompatible elements. Overturn is complicated but contains a strong spherical harmonic mode one component, as can be seen particularly in density field. Flow is dominantly downward along one axis and upward along the other. After overturn is nearly complete, attaining a nearly laterally uniform density, the temperature anomaly and the initial depth variable shows cool, incompatible element and Fe-rich material in a region of the upper mantle. Figure 3 shows this in more detail. This material remains near its depth and therefore is close to its solidus temperature.

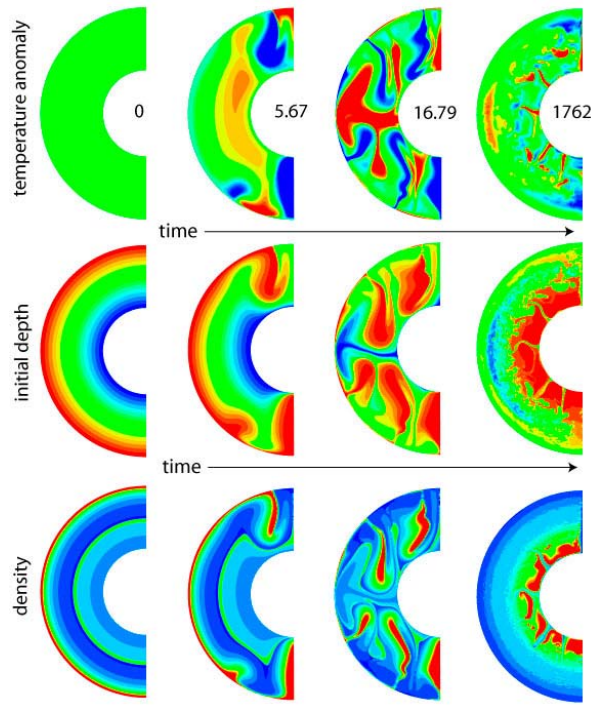

Figure 2: Overturn of an initially unstable density stratification like to that shown in Figure 1. Density (bottom), temperature anomaly (middle), and initial depth (top) are shown as functions of time normalized by the overturn time $t_{RT} = 4\pi\eta/(\Delta\rho g d^2)$ where d is the thickness of the silicate mantle, $\Delta\rho$ is the overall density difference, g is gravity, and η is the reference viscosity at the top of the mantle prior to overturn. Viscosity is a function of temperature and pressure. Overturn is rapid enough to be adiabatic. Temperature anomaly shows the deviation of from the azimuthally-averaged temperature at a given depth. Note that after overturn density approaches a laterally uniform structure while significant lateral heterogeneity in the initial depth variable persists indefinitely. These results were obtained using the CITCOM code [11].

Mantle evolution after overturn: The temperature in this region will increase as it gains heat conductively from surrounding warmer mantle and by radioactive decay of incompatible U, Th, and K. As it heats up, this material will rise only an amount $\rho\alpha\Delta T/(\partial\rho/\partial z)$ for which thermal expansion is balanced by the density change of surrounding stably stratified mantle. Thermally-driven convective overturn would require temperatures well above the melting temperature. Conductive heating to the temperature of adjacent mantle ($\Delta T \approx 300^{o}$C) will occur on a 100 Myr timescale. A temperature increase of only few hundred degrees should be enough to cause melting on this short time scale. The rate of radiogenic heating on longer timescales reflects the U, Th, and K concentration which depends strongly on the amount of intragranular melt previously trapped in the solid. Concentrations of 10x chondritic would result in a temperature rise of approximately 700°C after 1 Gyr. Melting should thus continue on Gyr timescales.

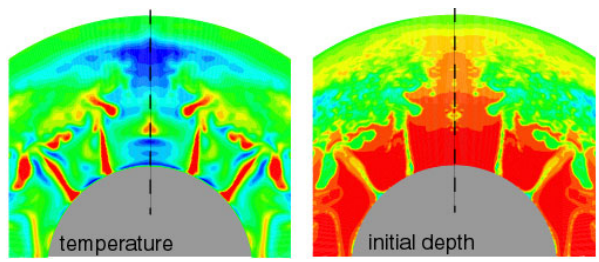

Figure 3. Temperature anomaly and initial depth at the final time shown in Figure 2.

On still longer timescales, heating of incompatible element-rich deep mantle, the material with a small initial depth in Figure 3, may cause convective instability. As shown by [10], local convective overturn and upward mixing of this dense region should occur. With strong compositional stratification (see Figure 1), thermal plumes are not expected to rise to the top of the mantle.

References: [1] Phillips, et al., Science 291, 2587-2591, 2001. [2] Zuber, M.T., et al., Nature 412, 220-227, 2001. [3] Johnson, C.L., and R.J. Phillips, LPSC 34, 1360, 2003. [4] Kiefer, W., MAP 39, 1815-32, 2003. [5] Harder, H. and U.R. Christensen, Nature 380, 507-509, 1996. [6] Reese, C.C., et al. J.G.R., 109, E08009, doi:10.1029/203JE002222, 2004. [7] Elkins-Tanton L.T., et al., MAP 38, 1753-1771, 2003. [8] Elkins-Tanton, L.T., et al., LPSC 34, 1479-1480, 2003. [9] Zaranek, S.E., et al. LPSC 35, 1642-43, 2004. [10] Alley, K.M., and E.M. Parmentier, PEPI 108, 15-32, 1998 [11] Zhong, S., personal communication, 2003.